Preparation and Characterization of TiO_2 and Polymer Nanocomposite Films with High Refractive Index

Norio Nakayama, Toyoharu Hayashi

R&D Center, Mitsui Chemicals, Inc., 580-32 Nagaura, Sodegaura-city, Chiba-ken 299-0265, Japan

Received 9 January 2007; accepted 23 February 2007
DOI 10.1002/app.26451
Published online 9 June 2007 in Wiley InterScience (www.interscience.wiley.com).

ABSTRACT: Novel nanocomposite films of TiO_2 nanoparticles and hydrophobic polymers having polar groups, poly (bisphenol-A and epichlorohydrin) or copolymer of styrene and maleic anhydride, with high refractive indices, high transparency, no color, solvent-resistance, good thermal stability, and mechanical properties were prepared by incorporating surface-modified TiO_2 nanoparticles into polymer matrices. In the process of preparing colloidal solution of TiO_2 nanoparticles, severe aggregation of particles can be reduced by surface modification using carboxylic acids and long-chain alkyl amines. These TiO_2 nanoparticles dispersed in solvents were found not to aggregate after mixing with polymer solutions. Transparent colorless free-standing films were obtained by drying a mixture of TiO_2 nanoparticles colloidal solution and polymer solutions in vacuum. Transmission electronic microscopic studies of the films suggest that the TiO_2 nanoparticles of 3–6 nm in diameter were dispersed in polymer matrices while maintaining their original size. Thermogravimetric analysis results indicate that the nanocomposite film has good thermal stability and the weight fraction of observed TiO_2 nanoparticles in the film is in good accordance with that of theoretical calculations. The refractive index of nanocomposite films of TiO_2 and poly(bisphenol-A and epichlorohydrin) was in the range of 1.58–1.81 at 589 nm, which linearly increased with the content of TiO_2 nanoparticles from 0 to 80 wt %. © 2007 Wiley Periodicals, Inc. J Appl Polym Sci 105: 3662–3672, 2007

Key words: nanocomposite films; TiO_2 nanoparticles; poly(bisphenol-A and epichlorohydrin)

INTRODUCTION

In recent years, inorganic/organic nanocomposites have attracted interest as new materials because they possess novel optical,[1–3] mechanical,[4] electronic,[5] gas barrier, and magnetic properties. In particular, the need for optical materials with high refractive index and transparency in the fields of optical waveguides,[1] ophthalmic lenses,[6] antireflection coatings, and adhesives for optical components is increasing.

Refractive indexes of conventional polymers are, even if high, limited to 1.6. To overcome this limitation high refractive index inorganic domain, such as TiO_2,[7] ZrO_2, SnO_2, CdS,[8] ZrS,[9,10] and PbS[11] have been introduced into polymer matrices. As preparation methods of inorganic/organic nanocomposites, two approaches have been known. The first method is to incorporate inorganic domains into polymer matrices using the sol-gel method. Many researchers successfully prepared inorganic/organic nanocomposites.[1–4,6–7,12–15] However, the inorganic domain in the composite obtained using this sol-gel method is amorphous[7] and the refractive index is relatively low in comparison with using nanoparticles. This is a disadvantage for preparing high refractive index composites. In addition, large shrinkage during the drying process may result in high inner stress inside the composite, leading to poor mechanical properties. Another method of fabricating high refractive index nanocomposites was developed by incorporating inorganic nanoparticles into polymer matrices. However, the optical scattering of inorganic particles, responsible for opacity, must be avoided for these composites. Small particles with diameters below one-tenth of the wavelength of visible light (400–800 nm) (typically < 25 nm), can avoid Rayleigh scattering and can be incorporated into a transparent polymer matrix to fabricate high refractive films of nanocomposites. A series of nanoparticles and polymer nanocomposites with high refractive indices have recently been prepared.[16–18] However, the polymers used in these studies are water-soluble polymers (hydrophilic polymers) and there is no chemical bonding or interaction between the nanoparticles and polymer matrix. Consequently, the application of such composite materials is restricted in the fields where materials with water insolubility, good thermal stability, and mechanical properties are required. TiO_2 may be a suitable inorganic component for increasing the refractive index of nanocomposites. TiO_2 exhibits a high refractive index ($n \sim 2.5$

Correspondence to: N. Nakayama (Norio.Nakayama@mitsui-chem.co.jp).

and 2.7, in the crystal forms of anatase and rutile, respectively). In this work, we synthesized TiO_2 nanoparticles[19] and modified the surface of TiO_2 using carboxylic acids and amines to disperse them into the polymer matrices without aggregation. We chose two hydrophilic polymers having polar groups: poly(bisphenol-A and epichlorohydrin) (PHE) and a copolymer of styrene and maleic anhydride (PSTMA). These polymers exhibit a high refractive index, good solvent-resistance, good thermal stability, and good mechanical strength.

EXPERIMENTAL

Materials

Titanium oxychloride ($TiOCl_2 \cdot xHCl \cdot H_2O$ (HCl: 38%–42% Ti: 15%)) was purchased from Fluka (Buchs, Switzerland). Propionic acid, *n*-propylamine, *n*-hexylamine, *n*-dodecylamine, were purchased as analytical grade reagents from Wako Pure Chemical Ind., Ltd. (Osaka, Japan) and used without further purification. Other chemical reagents were also obtained as analytical grade and used without further purification. Poly(bisphenol-A and epichlorohydrin) (PHE) (M_w: 40.000) and copolymer of styrene and maleic anhydride (PSTMA) (M_w: 224.000, maleic anhydride $\sim$ 7%), and polystyrene (PST) (M_w: 280.000) were purchased from Sigma-Aldrich (St. Louis, MO). Pellet PHE was dissolved in *N*,*N*-dimethylfolmamide (DMF), and then reprecipitated with methanol to remove extant epichlorohydrin. PSTMA and PST were used without further purification.

Methods

Synthesis of surface-modified TiO_2 nanoparticles

Synthesis of bare TiO_2 nanoparticles. Cosolvent of ethanol (600 mL) and distilled water (400 mL) were put into a three-necked round bottom flask fitted with a reflux condenser. Exactly 7.5 mL of titanium oxychloride (Ti^{4+}: $3.7 \cdot 10^{-2}$ mol) dissolved in 35 mL of distilled water was added drop wise to the reactor. The mixed solution was stirred under nitrogen flow at 60°C and it turned cloudy after $\sim$ 3 h. The precipitated solid was isolated as wet cake by centrifugation at 5000 rpm and it was washed five times with ethylacetate. After a small part of this solid was dried in evacuated desiccators, the X-ray powder diffraction (XRD) analysis of bare TiO_2 was performed.

Preparation of TiO_2 nanoparticles modified by propionic acid. In a typical preparation, isolated wet cake of a precipitated solid, without drying, was directly added in excess amount of propionic acid (50 mL). After stirring as slurry for 24 h at room temperature, the precipitate formed was collected as wet cake by centrifugation and washed five times with ethylacetate to remove the extra propionic acid. The wet cake of TiO_2 nanoparticles modified by propionic acid, without drying, was added to 50 g of cosolvent of *n*-butanol and toluene with a weight ratio of 1 : 1. In addition, it was sonicated for 1 h. The precipitated solid was perfectly dispersed into cosolvent of *n*-butanol and toluene. A colloidal solution of TiO_2 nanoparticles modified by propionic acid was obtained. (The content of TiO_2 nanoparticles modified by propionic acid in the colloidal solution was about 5 wt %. The solid part weight of TiO_2 nanoparticles was about 2.5 g. This value was estimated by evaporation desiccation.)

Preparation of TiO_2 nanoparticles modified by propionic acid and a variety of alkyl amines. Excess amount of each alkyl amine (10 mL): (i) not addition (as the comparison), (ii) *n*-propylamine, (iii) *n*-hexylamine, (iv) *n*-dodecylamine were added to each separately prepared colloidal solution (cosolvent of *n*-butanol and toluene) of TiO_2 nanoparticles modified by propionic acid. After stirring for 1 h, precipitated solids were obtained as wet cake by centrifugation and they were washed five times with ethylacetate to remove the extra amine. Each wet cake were added little by little to solvents as follows, (a) water, (b) 2-propanol, (c) chloroform, (d) toluene, and (e) THF, and they were sonicated for 1 h, and dispersibility was observed. Every dispersive property is summarized in Table I. The dispersibility of modified TiO_2 changed according to the length of an alkyl chain of each amine.

TABLE I
The Dispercive Property of TiO_2 Modified by Propionic Acid and a Variety of Alkyl Amines

	Solvents				
Amines	Water	2-propanol	Chloroform	Toluene	THF
1) Not addition	Dispersible[a]	Not[b]	Not	Not	Not
2) *n*-Propylamine	Dispersible	Dispersible	Not	Not	Not
3) *n*-Hexylamine	Not	Not	Dispersible	Not	Not
4) *n*-Dodecylamine	Not	Not	Dispersible	Dispersible	Partially dispersible[c]

[a] Dispersible: Colloidal dispersion was obtained (TiO_2: more than 5 wt % in solvent).
[b] Not: Colloidal dispersion was not obtained.
[c] Partially dispersible: Colloidal dispersion was obtained (TiO_2: less than 5 wt % in solvent or unstable).

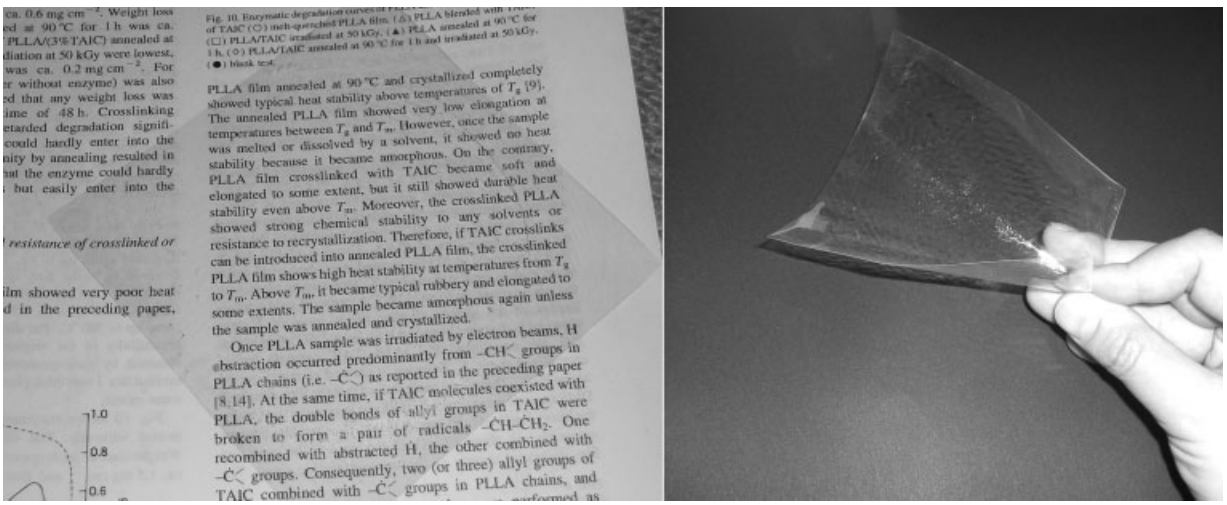

Figure 1 Photograph of the film of PHE-TiO_2(ca)-30 with 100–150 μm thickness.

Preparation of polymer/TiO_2 nanocomposite films

Preparation of PHE/TiO_2 nanocomposite films. (a) PHE/TiO_2 nanoparticles modified by propionic acid: In a typical preparation, 3.0 g of PHE was dissolved in 20 mL of cosolvent of *n*-butanol and toluene. The colloidal solution of TiO_2 nanoparticles modified by propionic acid in cosolvent of *n*-butanol and toluene was added to a polymer solution. The solid part weight of TiO_2 nanoparticles in cosolvent of *n*-butanol and toluene was checked beforehand by evaporative desiccation of a small part of colloidal solution. The TiO_2 content of films was controlled by changing the PHE/TiO_2 weight ratio. (PHE-TiO_2 (c)-*X* was defined as a film with *X* weight percent of TiO_2 modified by *c*arboxylic acid). Both polymer solution and TiO_2 solution were mixed by stirring until they became homogeneous under room temperature, and it was casted onto a petri dish (pure PHE and PHE-TiO_2 (c)-40). After the solvent was removed at 60°C for 12 h, free-standing films were peeled from the petri dish (thickness was adjusted to about 100–150 μm). The appearance of free-standing nanocomposite films were transparent, but stained strong yellow, without depending on the amount of TiO_2 nanoparticles.

(b) PHE/TiO_2 nanoparticles modified by propionic acid and *n*-hexylamine: PHE (3.0 g) was dissolved in 20 mL of chloroform. The colloidal solution of TiO_2 nanoparticles modified by propionic acid and *n*-hexylamine in chloroform was added to the polymer solution. The TiO_2 content of films was controlled by changing the PHE/TiO_2 weight ratio. (PHE-TiO_2 (ca)-*X* was defined as a film with *X* weight percent of TiO_2 modified by *c*arboxylic acid and *a*mine).

Both polymer solution and TiO_2 solution were mixed by stirring until they became homogeneous under room temperature and it was casted onto a petri dish (pure PHE, PHE-TiO_2 (ca)-10 to PHE-TiO_2 (ca)-40), and spin-coated on quartz plate (pure PHE, PHE-TiO_2 (ca)-10 to PHE-TiO_2 (ca)-80). After solvent was removed at 60°C for 12 h, free-standing films were peeled from the petri dish (thickness was adjusted to about 100–150 μm). Transparent and pliable films were obtained (Fig. 1). The films were not stained yellow, without depending on the amount of TiO_2 nanoparticles. The free-standing films were used at evaluations of thermogravimetric analysis (TGA), differential scanning calorimetric (DSC) analysis, thermomechanical analysis (TMA), transmission electronic microscopic (TEM) studies, mechanical properties, and solvent-resistance. The spin-coated films on quartz plate were used at evaluations of transmittance, refractive index, and so on.

Preparation of PSTMA/TiO_2 nanocomposite films. PSTMA (3.0 g) was dissolved in 20 mL of toluene. The colloidal solution of TiO_2 nanoparticles modified by propionic acid and *n*-dodecylamine in toluene was added to a polymer solution. The solid part weight of TiO_2 nanoparticles in toluene solution was checked beforehand by evaporation drying method (PSTMA-TiO_2 (ca)-*X* was defined as a film with *X* weight percent of TiO_2 nanoparticles modified by *c*arboxylic acid and *a*mine). After procedures used for PHE/TiO_2 nanocomposites, the films that were transparent and pliable were obtained.

Preparation of PST/nanocomposite/TiO_2 films. Procedures used for PSTMA/TiO_2 nanocomposites were performed. However, the nanocomposite films were translucent, without depending on the amount of TiO_2 nanoparticles.

Instrument and analytical procedures

Analysis of TiO_2 nanoparticles. After TiO_2 nanoparticles were synthesized by procedures shown above,

they were separated by centrifuging and dried in evacuated desiccators. The X-ray powder diffraction pattern was recorded using an X-ray diffraction meter (XRD: Model RINT2500 RIGAKU, Tokyo, Japan) with Cu Kα (λ = 1.5418 Å) radiation. TEM analyses were performed using a JEM-2010 (JEOL, Tokyo, Japan) operating at 100 or 120 kV. The water solution dispersing bare TiO_2 nanoparticles and the chloroform solution dispersing surface-modified TiO_2 nanoparticles were dried slowly on an amorphous carbon supported on a copper mesh TEM grid. The particle sizes of nanoparticles were determined by directly measuring them randomly chosen over 300 particles on the TEM images.

Adsorption of organic species on the TiO_2 nanoparticles was studied by Fourier transform infrared (FTIR) spectroscopy (Model FT/IR-300 JASCO, Tokyo, Japan) using the following preparative procedures. TiO_2 nanoparticles were dried in an oven at 120°C for 12 h, and then KBr pellets were prepared with the dried TiO_2 nanoparticles. The spectrum was collected in the range from 4000 to 500 cm^{-1}.

Analysis of nanocomposite film. The distributed state of TiO_2 nanoparticles in nanocomposite films was studied by TEM. Images were obtained using a JEM-2010 (JEOL) operating at 200 kV and H-7000 (HITACHI, Tokyo, Japan) operating at 80 kV. Samples were prepared for cross-sectional TEM observation by embedding the films in epoxy resin followed by curing and cutting the film surface using microtome with a diamond blade.

Transmission spectra of nanocomposite films were recorded on a UV–vis spectrophotometer using a UV-2200 (Shimadzu, Kyoto, Japan) in the range of 200–600 nm.

TGA was performed on a DTA-60 (Shimadzu) from 30 to 800°C at a heating rate of 10°C/min under nitrogen flow. DSC thermograms were performed on a DT-50 (Shimadzu) from 30 to 150°C at a heating rate of 10°C/min under nitrogen flow. TMA was used for evaluation of heat stability. A film 5 mm ×15 mm× about 100 μm (thickness) in size was fixed to the sample holder under a constant load of 3.0 g, then heated up to 200°C from 25°C with a heating rate of 10°C min^{-1} in a nitrogen atmosphere.

The refractive index of nanocomposite films was determined by the ellipsometric measurements using an M-150 (JASCO).

The tensile properties of the nanocomposite films were investigated on an instron tensile tester (Instron 1122) using a load of 20 kg. Test pieces of dumbbell form were fabricated from each film. Crosshead speed was 10 mm/min. The average of five tests was reported. The dynamic hardness of the nanocomposite films was investigated by an ultramicro hardness tester DUH-W201S (Shimadzu).

RESULTS AND DISCUSSION

Characterizations of TiO_2 nanoparticles modified by propionic acid and *n*-hexylamine

The XRD of bare TiO_2 nanoparticles is shown in Figure 2. These TiO_2 nanoparticles were formed to the anatase phase and average crystallite size was calculated as 3.3 nm from the peak of (101) reflection using Sherrer's equation.[20]

Sherrer's equation is as follows:

$$D = \frac{0.9\lambda}{\beta \cos\theta} \quad (1)$$

where D is the crystallite size, λ is wavelength of the radiation, θ is the Bragg's angle and β is the full width at half maximum.

Figure 3 illustrates the TEM micrographs of bare TiO_2 nanoparticles [Fig. 3(a,b)], TiO_2 modified by propionic acid and *n*-hexylamine, [Fig. 3(c,d)] and a size distribution [Fig. 3(e)]. The particles were spherical in shape with a narrow size distribution ranging from 2 to 6 nm. The average diameter of bare TiO_2 nanoparticles was 3.2 nm; it was in good agreement with the crystallite size calculated from XRD analysis. On the other hand, the average diameter of surface-modified TiO_2 nanoparticles was 3.9 nm. The size of surface-modified nanoparticles was, when compared with bare TiO_2 nanoparticles, same size or seemed to be slightly large.

FTIR spectrum of bare TiO_2 nanoparticles is shown in Figure 4(a). The peak at ~ 1620 cm^{-1} is attributed to absorbed water. FTIR spectrum of TiO_2 modified by propionic acid is shown in Figure 4(c). The peak of C—O stretching mode at 1720 cm^{-1} of propionic acid [Fig. 4(b)] splits to the asymmetric, $\nu_{as}(COO^-)$ and symmetric, $\nu_s(COO^-)$ bands, 1505 cm^{-1} and 1410 cm^{-1}, respectively. This indicates the formation of a chemical bond between the carboxylic group and the bronsted acid site (Ti—OH) of the TiO_2 surface.[20] FTIR spectrum of TiO_2 modified by propionic acid and *n*-hexylamine is shown in Figure 4(e). The peak at 1390 cm^{-1} is attributed to $\nu_s(CH_3)$

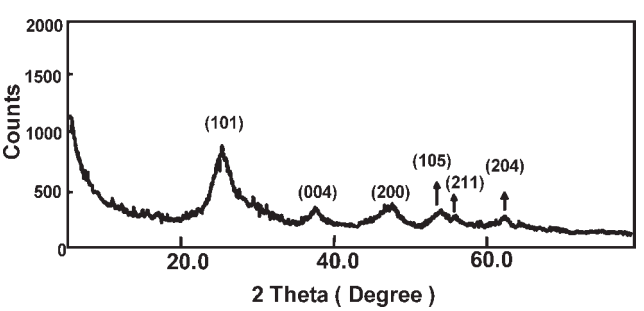

Figure 2 The XRD powder pattern of bare TiO_2 nanoparticles.

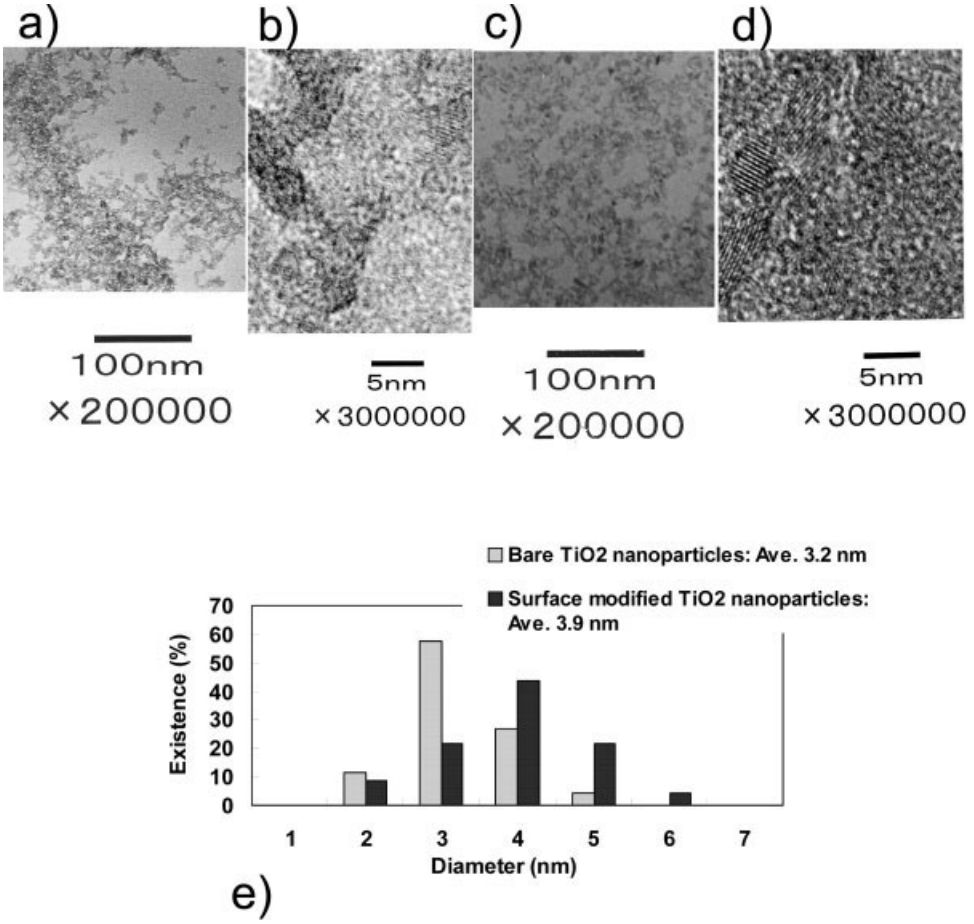

Figure 3 TEM micrographs of bare TiO_2 (a) ×200,000, (b) ×900,000 and surface-modified TiO_2, (c) ×200,000, (d) ×900,000, and (e) size distribution of bare TiO_2 and surface-modified TiO_2.

and the peak at 1460–1480 cm^{-1} is attributed to $\nu_{as}(CH_3)$ or $\nu(CH_2)$. In case of $\nu(NH_2)$ and $\nu(NH_2^+)$, it is supposed that they will appear in 1580–1650 cm^{-1} and 1560–1620 cm^{-1}, respectively, [Fig. 4(c,e)]. Two absorption regions are close to each other and overlap. Therefore, it is not clear which form of NH_2 or NH_2^+ amino groups take. Certain kinds of bond between amine and Lewis acid sites like Ti^+ on TiO_2 surface can be supposed[21] (Scheme 1).

In case of preparing the nanocomposite films using the TiO_2 nanoparticles modified by only carboxylic acid, the nanocomposite films stained strong

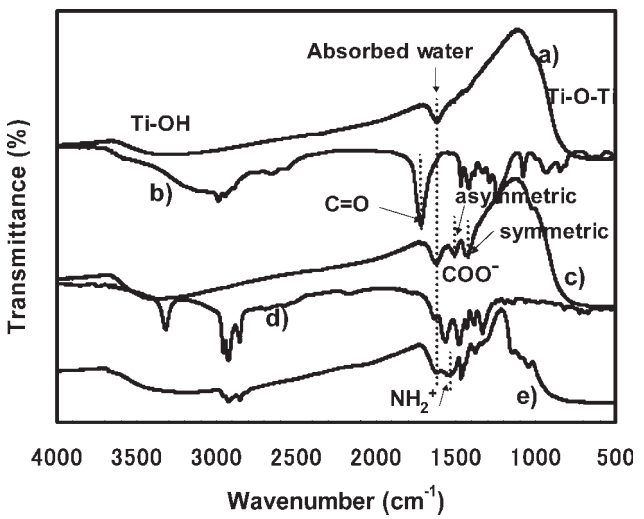

Figure 4 FTIR spectra of (a) bare TiO_2 nanoparticles, (b) propionic acid, (c) TiO_2 nanoparticles modified by propionic acid, (d) *n*-hexylamine, and (e) TiO_2 nanoparticles modified by propionic acid and *n*-hexylamine.

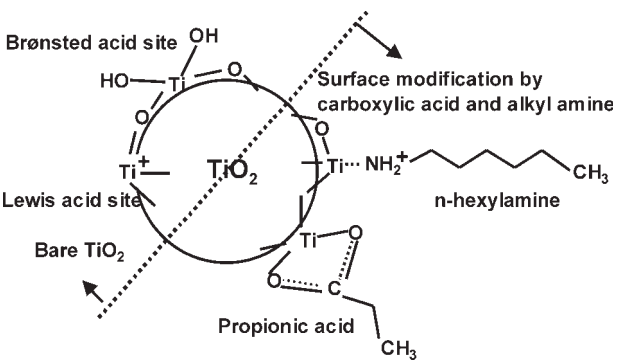

Scheme 1 Surface of TiO_2 nanoparticle modified by carboxylic acid and alkyl amine.

TABLE II
Color Change of Colloid Solution When Adding a Small Amount of Bisphenol-A or Anisole

TiO_2	Bisphenol A	Anisole
TiO_2 modified by propionic acid[a]	Strong yellow	Strong yellow
TiO_2 modified by propionic acid and *n*-hexyleamine[b]	No change	Very light yellow

[a] Co-solvent of *n*-butanol and toluene solution.
[b] Chloroform solution.

yellow. On the other hand, in case of preparing the nanocomposite films using TiO_2 nanoparticles modified by propionic acid and *n*-hexylamine, the yellow staining was not seen at all. To study this phenomenon, a simple practical experiment was performed as follows using bisphenol-A and anisole (the aromatic reagent with a lone electron pair—oxygen atom in a molecule). The color change of colloidal solutions of TiO_2 nanoparticles modified by only propionic acid or TiO_2 nanoparticles modified by propionic acid and *n*-hexylamine was observed, when adding a small amount of bisphenol-A or anisole. Table II summarizes these results. In case of TiO_2 nanoparticles modified by propionic acid only, the color of the colloidal solution becomes strong yellow. This phenomenon could be interpreted as follows. As mentioned above, because bisphenol-A and anisole are the aromatic reagents with a lone electron pair (oxygen atom in a molecule), the reagents would bind the Lewis acid site (Ti^+) onto the surface of the TiO_2 nanoparticle, and a dipole layer of bisphenol-A and anisole was formed toward the inner TiO_2 nanoparticle (Scheme 2). It was this dipole layer that induced an attracting potential for electrons inside the TiO_2 nanoparticle, which contributed to the reduction of the band gap of TiO_2, i.e., this layer introduced a red-shift tendency of the absorption band edge. The band structure of TiO_2 was mainly dependent on the crystal field effect, from which no pronounced change of band structure could be introduced by the surface dipole layer. However, the influence of the dipole on the binding energy of the exciton, i.e., the Coulomb interaction of electron and hold in TiO_2, were considerable. This layer might become the trap center of the exciton, which could enhance the exciton binding energy more significantly, and introduce a red shift of the absorption band edge of TiO_2, leading to yellow staining of the colloidal solution of TiO_2 nanopar-

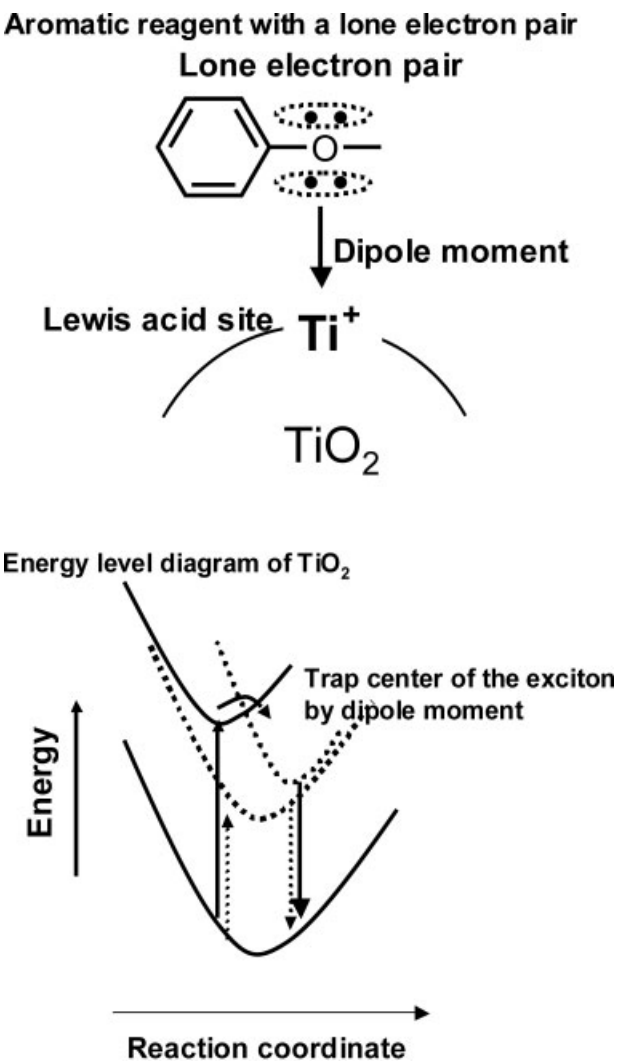

Scheme 2 One possibility of the mechanism of yellow coloring: interaction between the aromatic reagent with a lone electron pair (oxygen atom in a molecule) and the Lewis acid site (Ti^+) onto the surface of TiO_2.

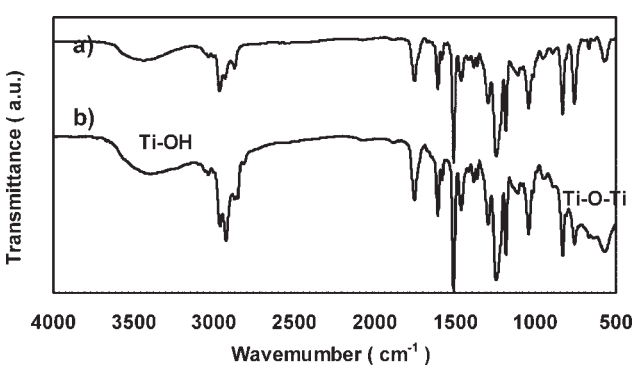

Figure 5 FTIR spectrum of (a) pure PHE and (b) PHE/TiO_2(ca) nanocomposite (PHE-TiO_2(ca)-30).

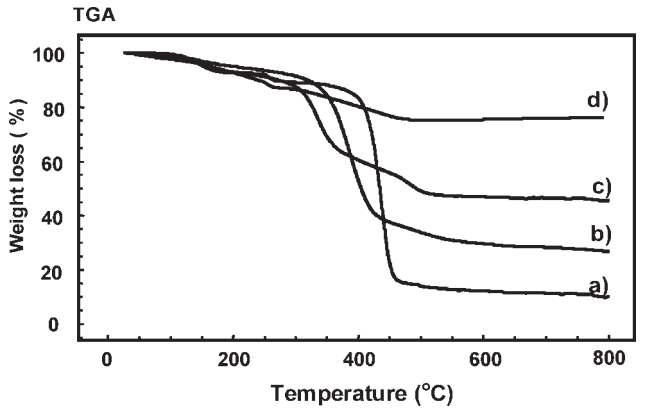

Figure 6 TGA curves of (a) pure PHE, (b) PHE-TiO_2(ca)-10, (c) PHE-TiO_2(ca)-40, and (d) TiO_2 nanoparticles modified by propionic acid and *n*-hexylamine.

ticles.[22] In case of TiO_2 nanoparticles modified by propionic acid and *n*-hexylamine, because the Lewis acid site (Ti^+) of the surface of TiO_2 is capped by alkyl amine, the interaction between TiO_2 and bisphenol-A or anisole was suppressed. So, the yellow staining of the colloidal solution of TiO_2 nanoparticles was suppressed.

Characterizations of polymer/TiO_2 nanocomposite films

In case of PHE-TiO_2 (c)-*X* (PHE/TiO_2 nanoparticles modified by propionic acid), strong yellow color was seen. On the other hand, in case of PHE-TiO_2 (ca)-*X* (PHE/TiO_2 nanoparticles modified by propionic acid *n*-hexylamine), the strong yellow color was not seen. The same phenomenon as studied by the TiO_2 and aromatic reagent with a lone electron pair was also seen in the case of PHE/TiO_2 nanoparticles modified by propionic acid, because the PHE had a lone electron pair and an oxygen atom part in the polymer structure.

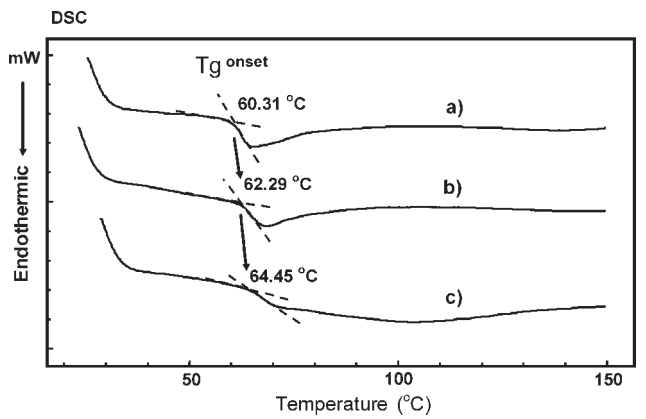

Figure 7 DSC curves of (a) pure PHE, (b) PHE-TiO_2(ca)-10, and (c) PHE-TiO_2(ca)-40.

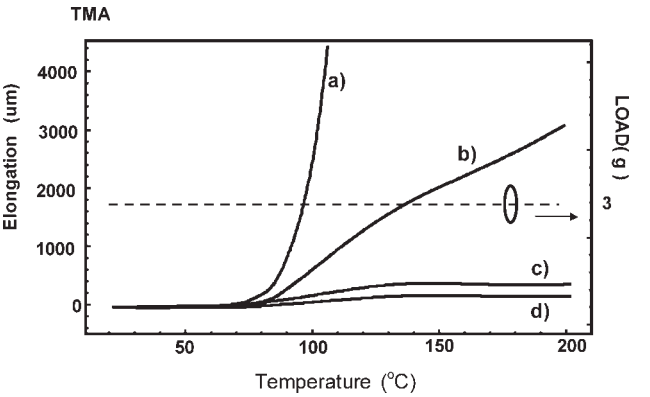

Figure 8 TMA heating curves: elongation of (a) pure PHE, (b) PHE-TiO_2 (ca)-10, (c) PHE-TiO_2 (ca)-20, and (d) PHE-TiO_2 (ca)-40 under the constant load (3 g) against temperature.

FTIR spectrum of the PHE/TiO_2 (ca) nanocomposite films is shown along with PHE in Figure 5. The broad absorption bands at 500–800 cm^{-1} correspond to (Ti—O—Ti) stretch peak [Fig. 5(b)]. The broad absorption bands at 3200–3500 cm^{-1} are for the Ti—OH residue group. The peaks of ν(—CH) stretch at 2900–3000 cm^{-1} were obviously increased, which resulted from the alkyl groups of *n*-hexylamine.

Figure 6 represents TGA curves of pure PHE, PHE-TiO_2 (ca)-10, and PHE-TiO_2 (ca)-40. Pure PHE has the initial decomposition temperature of 400°C. In case of nanocomposite films, the initial decomposition temperature shifted to lower temperatures with increasing TiO_2 contents in the film. PHE-TiO_2 (ca)-40 has two obvious weight loss regions: between 300 and 350°C, and from 450 to 500°C. The weight loss between 300 and 350°C can be attributed to the weight loss of the polymer matrix. The secondary weight loss at 450–500°C is attributed to the weight loss of surface modification compounds (propionic acid and *n*-hexylamine) on the surface of TiO_2 [Fig. 6(d)]. The residues of the nanocomposite films of PHE-TiO_2 (ca)-10 and PHE-TiO_2 (ca)-40 at 800°C are

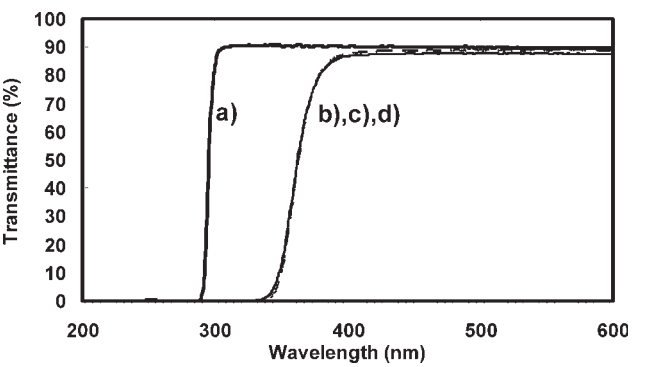

Figure 9 The transmittance spectra of (a) pure PHE, (b) PHE-TiO_2 (ca)-50, (c) PHE-TiO_2 (ca)-60, and (d) PHE-TiO_2 (ca)-70 (PHE-TiO_2 (ca)-50 to 70 overlaps together).

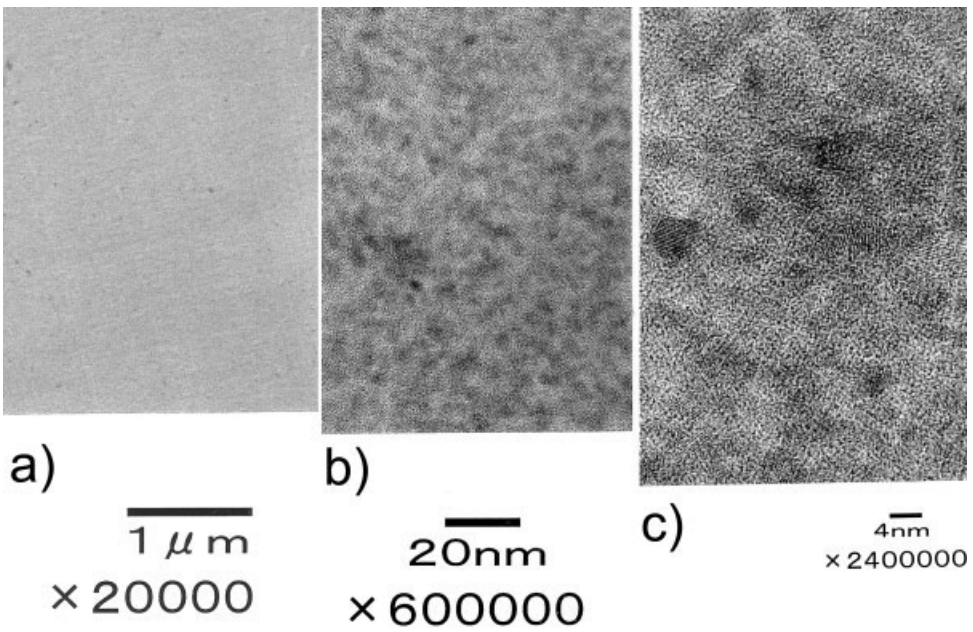

Figure 10 TEM micrographs of the nanocomposite film of PHE-TiO_2 (ca)-40 (a) ×2000, (b) ×600,000, and (c) ×2400,000.

in the range of 28.0%–46.4% and they increase with an increase of TiO_2 contents in the films.

Figure 7 represents DSC curves of pure PHE, PHE-TiO_2 (ca)-10, and PHE-TiO_2 (ca)-40. The pure PHE polymer exhibits a glass transition temperature (T_g) at about 65°C. PHE-TiO_2 (ca)-10 and PHE-TiO_2 (ca)-40 have also a T_g, however, they slightly shifted to high temperature and changed to a small peak with increasing TiO_2 contents.

Figure 8 shows TMA heating curves, i.e., elongation of pure PHE, PHE-TiO_2 (ca)-10, PHE-TiO_2 (ca)-20, and PHE-TiO_2 (ca)-40 under the constant load (3 g) against temperature. The pure PHE began to elongate at 80°C and elongate significantly at 90°C.

The PHE-TiO_2 (ca)-10 started to elongate at 80°C, however it elongated gradually above 90°C. The PHE-TiO_2 (ca)-20 showed heat resistance until 200°C, though it elongated with the steepest slope above 80°C.

The results of DSC and TEA suggest that nanocomposite films have higher rigidity due to the incorporation of TiO_2 nanoparticles, which restrict the motion of the polymer chain segments.

Optical transparency of nanocomposite films with a thickness of about 1 μm on the quartz plates, using a quartz plate as reference, was characterized by UV–vis spectra. Figure 9 shows the transmittance spectra of pure PHE and PHE-TiO_2 (ca)-50 to 70 (PHE-TiO_2 (ca)-50 to 70 overlap together). It was observed that transmittance of the nanocomposite film is above 85% and similar to pure PHE in the region from 400 to 600 nm, although it falls by absorption of TiO_2 nanoparticles on a wavelength of below 400 nm. This

TABLE III
Refractive Index Change of PHE/TiO_2 and PSTMA/TiO_2 Films as a Function of Modified TiO_2 Weight

Film	Ellipesometry, n_{589}	Film	Ellipesometry, n_{633}
Pure PHE	1.58	Pure PSTMA	1.57
PHE-TiO_2 (ca)-10	1.60	–	–
PHE-TiO_2 (ca)-20	1.63	–	–
PHE-TiO_2 (ca)-30	1.65	–	–
PHE-TiO_2 (ca)-40	1.68	PSTMA-TiO_2 (ca)-40	1.64
PHE-TiO_2 (ca)-50	1.70	–	–
PHE-TiO_2 (ca)-60	1.73	PSTMA-TiO_2 (ca)-60	1.70
PHE-TiO_2 (ca)-70	1.76	PSTMA-TiO_2 (ca)-70	1.74
PHE-TiO_2 (ca)-80	1.81	PSTMA-TiO_2 (ca)-80	1.76

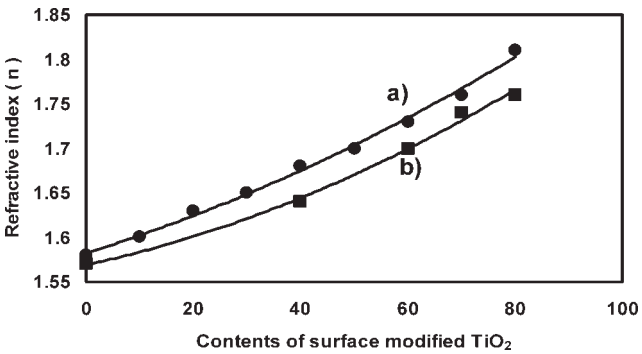

Figure 11 Refractive index increases with the weight content of the surface-modified TiO_2 nanoparticles (a) PHE-TiO_2 (ca)-X and (b) PSTMA-TiO_2 (ca)-X.

TABLE IV
Mechanical Properties of PHE/TiO_2 Nanocomposite film

Films	Thickness (μm)	Tensile properties[a]			Dynamic hardness[e] (GPa)
		YM[b] (GPa)	TS[c] (MPa)	EB[d] (%)	
Pure PHE	110	2.7	45.2	2.5	14.5
PHE-TiO_2 (ca)-10	117	2.8	55.4	2.8	—
PHE-TiO_2 (ca)-20	130	3.2	58.4	2.6	—
PHE-TiO_2 (ca)-30	121	3.5	62.1	2.1	19.2
PHE-TiO_2 (ca)-40	112	—	—	—	20.7

— Indicates that the average of five tests was reported.
[a] The tensile properties of the nanocomposite films were investigated on a universal tensile tester.
[b] Young's modulus.
[c] Tensile strength at break.
[d] Elongation percentage at break.
[e] The dynamic hardness of the nanocomposite film was investigated on a dynamic ultramicro hardness tester.

TABLE V
Solvent-Resistance of PHE/TiO_2 Nanocomposite film

Films	Solvents			
	Toluene	Chloroform	Acetone	Methanol
Pure PHE	Slight dissolution	Dissolution	Dissolution	No change
PHE-TiO_2 (ca)-10	No change	No change	No change	No change
PHE-TiO_2 (ca)-20	No change	No change	No change	No change
PHE-TiO_2 (ca)-30	No change	No change	No change	No change
PHE-TiO_2 (ca)-40	No change	No change	No change	No change

Solvent-resistance was examined by rubbing with tissue paper solvent was damped.

result suggests that the TiO_2 nanoparticles are uniformly distributed in the films.

Figure 10 illustrates the TEM micrograph of the nanocomposite films of PHE-TiO_2 (ca)-40.The TiO_2 nanoparticles of 3–6 nm sizes were uniformly dispersed into the polymer matrices without aggregation after immobilization into the polymer matrix.

The pure PHE has a high refractive index (1.58), and it is a preferred candidate for polymer matrix for fabrication of high refractive index nanocomposites (similarly, the pure PSTMA has the high refractive index). The bulk TiO_2 exhibits a higher refractive index, anatase as $\sim$ 2.5, and the incorporation of surface-modified TiO_2 particles into the PHE matrix results in an increase in the refractive index of the nanocomposite films. In case of PHE-TiO_2 (ca) nanocomposites, when the content of surface-modified TiO_2 is above 80 wt %, nanocomposite films (>1 μm thickness) with good mechanical properties cannot be obtained. So here, we only prepared nanocomposite films with the content of surface-modified TiO_2 below 80 wt %. The refractive index increases linearly from 1.58 to 1.81 with the weight content of the surface-modified TiO_2 nanoparticles (in case of PSTMA/TiO_2 (ca) nanocomposites, the refractive index increase linearly from 1.57 to 1.76) (Table III, Fig. 11).

Tensile properties and dynamic hardness were taken into account as mechanical properties. The dependence of Young's modulus (YM), tensile strength (TS) at break, and dynamic hardness on nanocomposite films is summarized in Table IV, Obviously, YM, TS at break, and dynamic hardness were higher than

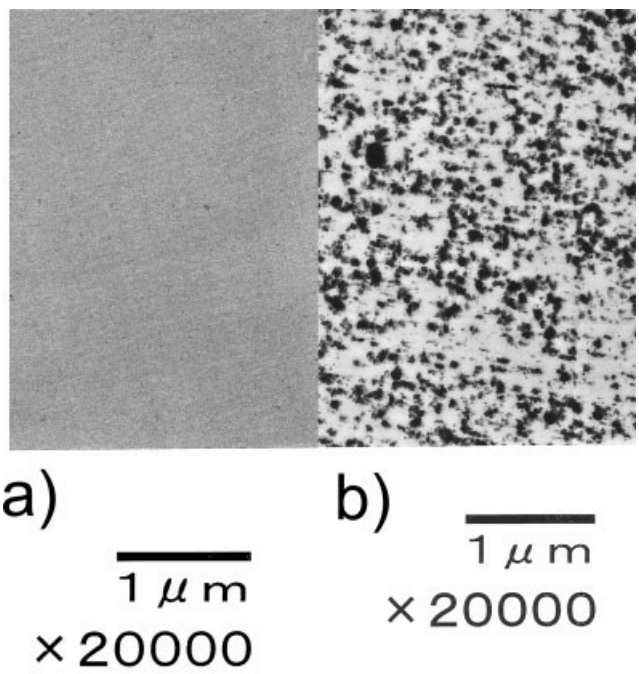

Figure 12 TEM micrographs of the nanocomposite film of (a) PSTMA-TiO_2 (ca)-40 and (b) PST-TiO_2 (ca)-40.

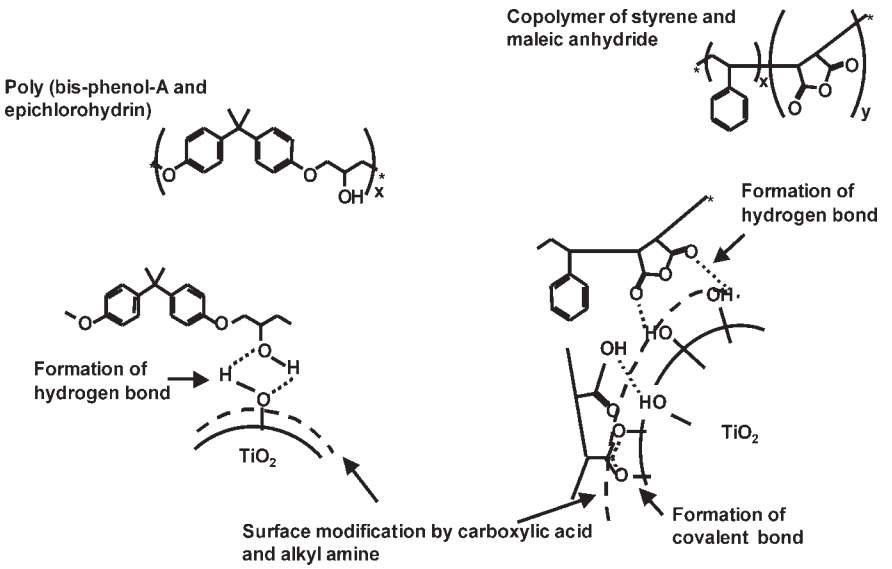

Scheme 3 One possibility of interactions between polymer and TiO_2 nanoparticles (carboxylic acid and amine of surface modification agent of TiO_2 were omitted in this scheme to make it plain).

those of the pure PHE. YM and TS at break increased with TiO_2 nanoparticles contents.[4] However, when content was about 40 wt % or more, the test piece of the film can be fabricated, but they were too fragile to attach in the instron tensile tester. Therefore, the measurement of the tensile properties of the films containing below 30 wt % TiO_2 nanoparticles was performed.

Solvent-resistance of PHE/TiO_2 nanocomposite films is summarized in Table V. Solvent-resistance was examined by rubbing with solvent-soaked tissue paper. As for pure polymer, it showed poor solvent-resistance, especially for acetone, toluene, and chloroform. On the other hand, nanocomposite films showed good solvent-resistance. In addition, they did not depend on the amount of TiO_2 nanoparticles.

Figure 12 illustrates the TEM micrographs of the nanocomposite films of PSTMA-TiO_2 (ca)-40 or PST-TiO_2 (ca)-40. In case of PSTMA-TiO_2 (ca)-40, the TiO_2 nanoparticles was uniformly dispersed into the polymer matrix, and the aggregation of TiO_2 nanoparticles was not observed, like PHE. On the other hand, in case of PST-TiO_2 (ca)-40, TiO_2 nanoparticles form a two-dimensional aggregation in the polymer matrix, and submicron-sized particles were observed.

TiO_2 has residual activity sites: bronsted acid site (Ti—OH) or Lewis acid sites like Ti^+, also after the surface is modified by carboxylic acid and amine. Since the polymers with polar groups like PHE, PSTMA have an interaction, for example, a hydrogen bond, a covalent bond, with active sites of TiO_2 (Scheme 3), TiO_2 nanoparticles do not form aggregation in polymer matrices when removing the solvent (although it was not always clear from analysis of FTIR). On the other hand, since the polymers without polar groups like PST do not have an interaction with the surface of TiO_2, TiO_2 nanoparticles will form aggregation when removing the solvent.[23]

CONCLUSIONS

In conclusion, by effective surface modification of TiO_2 nanoparticles using carboxylic acid and long-chain alkyl amine, a colloidal solution of TiO_2 nanoparticles can be obtained. By the interaction between TiO_2 and polar groups in the polymer, the dispersion of TiO_2 nanoparticles can be controlled in the polymer matrix.

TEM studies suggest that the TiO_2 nanoparticles with an average diameter of 3–6 nm are uniformly dispersed in the polymer matrix. The nanocomposite films exhibit excellent optical transparency in the visible region and have a high refractive index, which corresponds to the content of the TiO_2 in the films. These nanocomposite materials may be suitable as industrial high refractive index films and for optical coatings.

This work was carried out under the research and development at Mitsui Chemicals, Inc., Japan. The authors thank Mr. Atsuo Otuji, Mr. Hiroshi Naruse for fruitful discussions and suggestions.

References

1. Yoshida, M.; Prasad, P. N. Chem Mater 1996, 8, 235.
2. Zhang, J.; Wang, B.-J.; Ju, X.; Hu, T.-D. Polymer 2001, 42, 3697.
3. Zhang, J.; Ju, X.; Li, Q.-U.; Liu, T.; Hu, T.-D. Synth Met 2001, 118, 181.

4. Nakane, K.; Kurita, T.; Ogihara, T.; Ogata, N. Compos B Eng 2004, 35, 219.
5. Su, S.-J.; Kuramoto, N. Synth Met 2000, 114, 147.
6. Müller, P.; Braune, B.; Becker, C.; Krug, H.; Schmidt, H. Proc. SPIE-Int Soc Opt Eng 1997, 3136, 462.
7. Lü, C.; Cui, Z.; Guan, J.; Yang, B.; Shen, J. Macromal Mater Eng 2003, 288, 717.
8. Wang, J.; Montville, D.; Gonsalves, K. E. J Appl Polym Sci 1999, 72, 1851.
9. Lü, C.; Cui, Z.; Yang, B.; Shen, J. J Mater Chem 2003, 13, 526.
10. Lü, C.; Cui, Z.; Wang, Y.; Li, Z.; Guan, C.; Yang, B.; Shen J. J Mater Chem 2003, 13, 2189.
11. Lü, C.; Cui, Z.; Liu, Y.; Cheng, Y.; Yang, B. Chem Mater 2005, 17, 2448.
12. Hu, Q.; Marand, E. Polymer 1999, 40, 4833.
13. Wang, B.; Wilkes, G. L.; Hedrick, J. C.; Liptak, S. C.; Mcgrath, J. E. Macromolecules 1991, 24, 3449.
14. Coltrain, B. K.; Landry, C. J. T.; Sedita, J. S.; Kelts, L. W.; Landry, M. R.; Long, V. K. Chem Mater 1993, 5, 1445.
15. Chan, C.-K.; Peng, S.-J.; Chu, I.-M.; Ni, S.-H. Polymer 2001, 42, 4189.
16. Zimmerman, L.; Weibel, W. J Mater Res 1993, 8, 1742.
17. Nussbaumer, R. J.; Caseri, W. R. Macromol Mater Eng 2003, 288, 44.
18. Papadimitrakopoulos, F.; Wisniecki, P.; Bhagwagar, C. E. Chem Mater 1997, 9, 2928.
19. Kim, S.-J.; Park, S.-D.; Jeong, Y.-H. J. J Am Ceram Soc 1999, 83, 927.
20. Ojamäe, L.; Aulin, C. J Colloid Interface Sci 2006, 296, 71.
21. Okazaki, S.; Kuramochi, K. Chem Soc Japan 1982, 7, 1141.
22. Zhao, J.; Lai, Z. Appl Phys Lett 1991, 59, 1826.
23. Weng, C.-C.; Wei, K.-H. Chem Mater 2003, 15, 2936.